International Journal of Information Acquisition
Vol. 3, No. 4 (2006) 339–347

World Scientific
www.worldscientific.com

THE BOND STRENGTH MEASUREMENT OF SILICON-SILICON BONDING WAFERS BASED ON CRACK OPENING METHOD

LIGUO CHEN, TAO CHEN and LINING SUN
Robotics Institute, Harbin Institute of Technology
Harbin, Hei Long Jiang, 150080, China

Received 8 August 2006
Accepted 14 March 2007

A measurement system based on crack-opening method has been developed to measure the fracture toughness of silicon direct bonding wafers. The theory of crack-opening method was introduced and amended according to the shape of the specimen. The parameters and function required in the measurement of bond energy were mentioned, and the selection principle of thickness of the razor was given. A new experimental device based on IR vision and image processing in the measurement was developed. Finally, a contrast experiment was carried out successfully and the error of the method was analyzed which validated the feasibility and the localization of the method.

Keywords: Bonding strength; wafer bonding; surface energy; crack-opening.

1. Introduction

Silicon direct wafer bonding or fusion bonding is an attractive technology for the realization of three-dimensional microstructures for micromachined devices, smart sensors, actuators and optoelectronic components. Separately processed wafers are bonded together which provide better process and structure flexibility than monolitic integration.

Different methods of mechanical testing of bonding interfaces are known [Tong & Gösele, 1999; Lasky, 1986; Barth, 1990]. Bond strength can be tested by the pull-test method, in which bonded wafers are pulled apart from two opposite direction perpendicular to the bonded surface to separate the bonded pieces [Tong & Gösele, 1999; Lasky, 1986; Barth, 1990]. Besides the pull-test method, "crack-opening" (so-called Maszara test [Lasky, 1986] is also used for bond strength measurements [Tong & Gösele, 1999; Lasky, 1986; Barth, 1990]. Pull-test methods cannot be used because they do not measure surface energy — instead they measure the tensile strength which strongly depends on microcracks and sample preparations. The crack-opening method is based on wafer pair debonding, that is initiated by inserting a separating material such as a razor blade between bonded wafers. Wafer debonding area correlates to the equilibrium between elastic forces of the separated wafers and bonding forces at the crack tip. Crack-opening methods utilize

measurement of bond energy associated with interaction energy of bonded surfaces per unit area. If bond energy value approaches the surface energy of the wafer material, wafer fracture usually takes place. Because of that, not one of the above methods can be directly applied for characterization of commercially used DWB-technologies.

In this paper, the theory of crack-opening method was introduced and amended according to the shape of the samples usually used. Through analysis of the method, the parameters and function required in the measurement of bond energy were mentioned. A new experimental device based on IR vision and image processing in the measurement was developed. And a contrast experiment was carried out successfully and the error of the method was analyzed.

2. Theory of Crack Opening Method

The bonding energy may be characterized by the energy associated with opening the surface by the so-called crack-opening method first described by Maszara in 1986 [Tong, 2001; Tvergaard & Hutchinson, 2006]. But it was too difficult to actualize, so it did not have a broad application. The relevant approach for characterizing interface toughness is to work within the framework of fracture mechanics and to measure the critical energy release rate G_c, i.e. the "bond fracture toughness". G_c is equal to twice the surface energy γ only in the case of brittle materials or bonds in which no other mechanism than atomic planes separation takes place. When, for instance, friction occurs between crack faces or dislocations are emitted at the crack tip, G_c becomes significantly larger than 2γ. When G_c equals 2γ, the crack tip are in unstable equilibrium.

Simple beam theory leads to the following relationship between the crack length and the toughness for the configuration presented in Fig. 1, where L is the crack length, γ is the surface energy that defined in term of the parameters E, t_w, t. E_1, and E_2 are known as the Young's modulus number. The parameters t_{w1}, t_{w2} are the thickness of the bonded wafers, and t_b is the thickness of a blade.

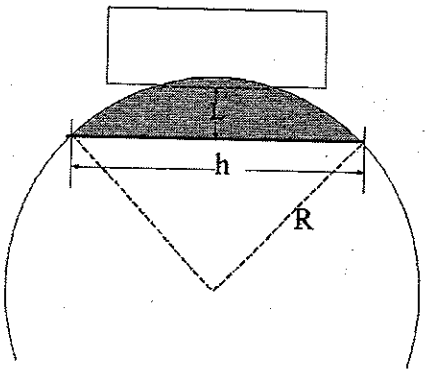

Fig. 1. Crack-opening method.

The inertia moment of crack part is

$$I_i = \frac{b_i^3 h}{12} \quad (i = 1, 2). \tag{1}$$

The bending force can be described in Eq. (2) as:

$$t_i = \frac{F_i L^3}{3E_i I_i} \quad (i = 1, 2), \tag{2}$$

and it can be found from Eq. (3) as:

$$F_i = \frac{E_i h b_i^3 t_i}{3E_i I_i}, \quad (i = 1, 2). \tag{3}$$

From the theory of Clapeyron, elasticity deformation energy is

$$U_T = \frac{1}{2}F_1 t_1 + \frac{1}{2}F_2 t_2 = \frac{F_1^2 L^3}{6E_1 I_1} + \frac{F_2^2 L^3}{6E_2 I_2}. \tag{4}$$

So, the total energy equation of system is

$$U = U_T + (\gamma_1 + \gamma_2)S. \tag{5}$$

S is the area of crack part, the gray area in Fig. 1 is the crack part. S can be calculated as

$$S = R^2 \cdot \arccos\frac{R - L}{L} - \frac{h \cdot (R - L)}{2}. \tag{6}$$

The total energy U can be described as

$$U = \frac{hE_1 b_1^3 t_1^2 + hE_2 b_2^3 t_2^2}{8L^3} + (\gamma_1 + \gamma_2) \times \left(R^2 \cdot \arccos\frac{R - L}{L} - \frac{h \cdot (R - L)}{2}\right), \tag{7}$$

where $h = 2\sqrt{2RL - L^2}$.

Solving for U result in

$$U = \frac{\sqrt{2RL - L^2}}{4L^3}(E_1 b_1^3 t_1^2 + E_2 b_2^3 t_2^2) + (\gamma_1 + \gamma_2) \cdot \left(R^2 \cdot \arccos \frac{R-L}{R} - (R-L)\sqrt{2RL - L^2} \right). \tag{8}$$

The condition of force balance is

$$\frac{\partial U}{\partial L} = 0. \tag{9}$$

Substituting Eq. (10) into Eq. (11) results in

$$\frac{2L - 5R}{4L^4\sqrt{2RL - L^2}}(E_1 b_1^3 t_1^2 + E_2 b_2^3 t_2^2) + (\gamma_1 + \gamma_2)(2\sqrt{2RL - L^2}) = 0. \tag{10}$$

So

$$(\gamma_1 + \gamma_2) = \frac{5R - 2L}{8L^3(2RL - L^2)}(E_1 b_1^3 t_1^2 + E_2 b_2^3 t_2^2) = \frac{5R - 2L}{16RL^4 - 8L^5}(E_1 b_1^3 t_1^2 + E_2 b_2^3 t_2^2). \tag{11}$$

The average surface energy of bonded wafers is

$$\gamma = \frac{5R - 2L}{32RL^4 - 16L^5}(E_1 b_1^3 t_1^2 + E_2 b_2^3 t_2^2). \tag{12}$$

As for wafer-to-wafer bonding with the same thickness wafers, $t_{w1} = t_{w2} = t$, $E_1 = E_2 = E$, and suppose that $b_1 = b_2 = b$, Eq. (12) can be simplified as

$$\gamma = \frac{(5R - 2L)Eb^3t^2}{64RL^4 - 32L^5}. \tag{13}$$

The razor blade used in the measurement is quadrate but wafer is round in shape. After the razor is inserted, the wafer gets imbalance force along the line of the edge of razor. The finite element analysis (shown in Fig. 2) indicates that the force along the edge of razor descend from middle to side. So the bottom of the crack is not an ideal line but a curve as shown in Fig. 3.

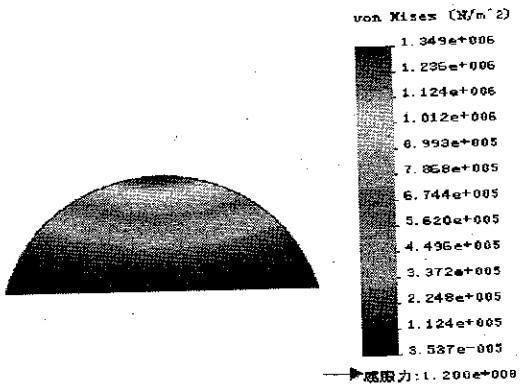

Fig. 2. Finite element analysis of crack-opening process.

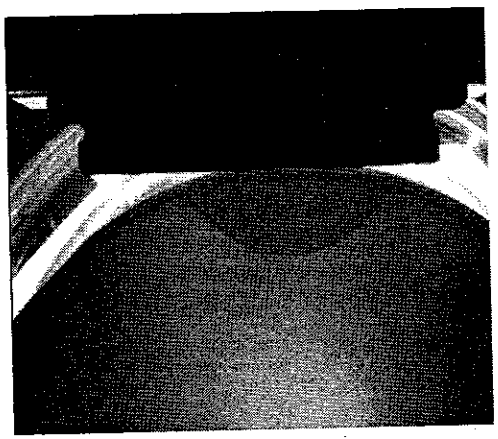

Fig. 3. Crack-opening line.

Thus, equation educed by crack-opening method should be amended. Suppose λ is the ratio of the areas of the real wafer crack and the theoretical crack, then,

$$U = \frac{hE_1 b_1^3 t_1^2 + hE_2 b_2^3 t_2^2}{8L^3} + (\gamma_1 + \gamma_2)\lambda \times \left(R^2 \cdot \arccos \frac{R-L}{L} - \frac{h \cdot (R-L)}{2} \right). \tag{14}$$

Using the uniform principle, the average surface energy of bonded wafers can be described as:

$$\gamma = \frac{(5R - 2L)Eb^3t^2}{\lambda(64RL^4 - 32L^5)}. \tag{15}$$

The strength of wafer bonding can be calculated as long as the area of the crack part can be measured using image processing.

In the crack opening progress, the capability of the razor is important and pivotal. It is determinant to the result of the experiment. The razor has three factors, the thickness, the length and the width. Different bonding strength will bring different inserting result. The weak strength is advantageous to the inserting, and the crack appears easily under the infrared light. However, if the bonding strength of the wafers is strong, the indexes of the razor should be calculated or tested. Otherwise the razor will be bended or the edges of wafers will be broken (shown in Fig. 4).

Before the calculation and test of the razor, the edge of the actual wafers should be described. For the influence of the process and surface treating, the edge of the wafer is a dent or round angle. When the wafers are bonded together, the edge of the wafers bring out a V-shaped joint. It is called pre-crack. The joint is convenient for the inserting of the razor.

If the intensity of the razor is enough, the thickness of the blade decides the result of the test. At first, the wafers in crack-opening area can be supposed as two cantilevers, the thickness of the blade is the sum of the flexivities of the cantilevers. So the Third Strength Theory in mechanics of material can be used to analyze the thickness of the blade when the edges of the wafers are broken:

$$\frac{M}{W_z} \leq [\sigma], \tag{16}$$

where M is the moment, W_z is the bending modulus, and $[\sigma]$ is admissible stress.

A too thick blade will break the wafers. Combining the theory and the test, the thickness of the blade under 200 μm is availability.

If the thickness of the blade is too thin, it will be invalidation. Here the stability theory of the pressure bar in mechanics of material can be used to analyze the thickness of the blade when the blade is invalidation:

$$F \leq \frac{\pi^2 EI}{(2l)^2}, \tag{17}$$

where l is the length of the blade, E is the Young's modulus number, and F is stress on the blade. Combining the theory and the test, the thickness of the blade above 100 μm is availability.

3. System Architecture

Section 2 described the principle of crack-opening method. From the conclusion of the analysis, the measurement system must have two functions. One is to measure the thickness of the blade and the wafers, and the crack length. The other is to align the blade to the wedge between wafers and insert it to create crack.

In order to achieve the function needed, the system is comprised of several subsystems as Fig. 5. The subsystems include:

(1) Positioning subsystem,
(2) vision subsystem,
(3) accessorial subsystem.

The positioning subsystem is consists of two positioning modals. One is to adjust the wafer to align with the blade, and the other modal drive the blade inserting into the wedge between wafers.

Microscopic subsystem will measure the thickness of the wafer and the blade, and guide the alignment motion. The infrared subsystem will measure the crack length. The assistant subsystem includes the wafer clamper, the blade, and other accessory components.

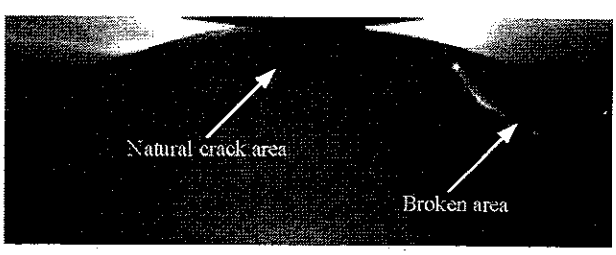

Fig. 4. Broken edge in the test.

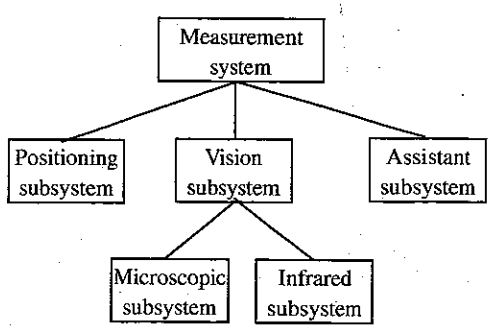

Fig. 5. Architecture of the measurement system.

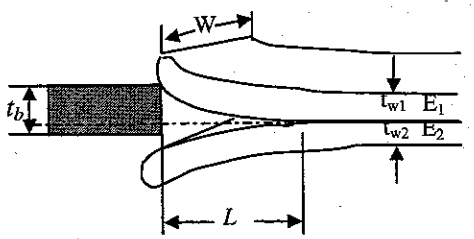

Fig. 6. Crack-opening when misalignment.

3.1. *Positioning subsystem*

Indeed, small misalignment of the razor blade with respect to the crack plane leads to an effective opening that can be significantly larger than the blade thickness as shown in Fig. 6. The error can be very important as γ is proportional to the square of the effective opening t_b (see Eq. (2)). The specimen must be mounted on a free rotation clamper, which mounted on a precision positioning worktable named wafer adjustment stage to allow perfect alignment of the blade during testing. On the other hand, the inserting depth of the blade should be precisely controlled by another positioning modal named razor feeding stage to avoid damage to the specimen during testing.

Usually, the thickness of wafers we used is about 100 μm–600 μm, and there is a pre-crack between wafers after bonding. In order to assure the precisely alignment, the positioning stages of this system are actuated by precision stepmotors. The specification of them is shown in Table 1.

Table 1. Specification of positioning stages.

Classification	Specification		
	Range (mm)	Resolution (μm)	Positioning accuracy (μm)
Wafer adjustment stage	100	0.1	0.5
Razor feeding stage	70	0.1	0.5

3.2. *Microscopic subsystem*

3.2.1. *Components*

In order to recognize the thickness of the blade and wafers and monitor the testing process, the author used one optical microscope vertically to the crack plane. The vision system consists of a 1/2″ CCD camera, a zoom lens with long working space that can provide magnification from 1.0X to 12X, an interface card and a LED light source.

3.2.2. *Alignment*

Another task of microscopic subsystem is to align the razor blade with respect to the crack plane. Usually, after wafer-to-wafer bonding, there is a pre-crack between wafers as Fig. 7. The edge image of the razor and the wafer was gained using canny arithmetic, then the razor blade and the crack line can easily obtained by image processing and marked with dashed line.

3.3. *Infrared subsystem*

The crack length and area can be continuously measured owing to the IR transparency of silicon and the contrast resulting from the presence of air between the wafers [Lawn, 1993; Maszara *et al.*, 1998].

The infrared system consists of an IR source and an IR sensitive camera. A silicon charge-coupled device camera has sufficient sensitivity in the near-IR range that it can be used when outfitted with a filter for visible light. The bonded wafer pair is located between the source

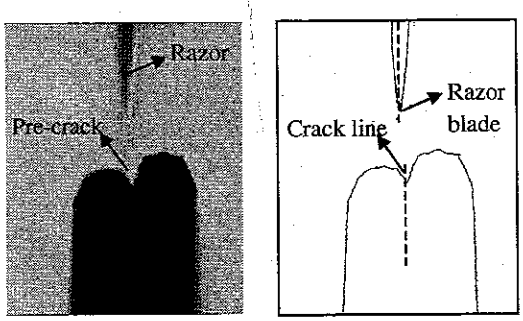

Fig. 7. Microscopic image of razor and wafer and measurement of alignment parameter.

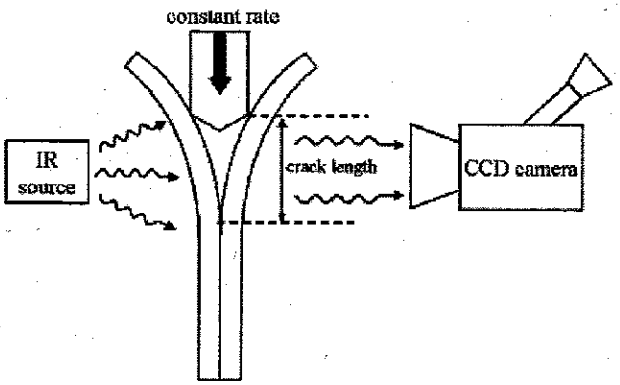

Fig. 8. Measurement principle of crack length.

and camera as shown in Fig. 8. The crack created by the blade shows up as changes in contrast in the IR image. Large unbonded or crack regions appear with a characteristic "Newton's Rings" interference pattern [Piotrowski & Jung, 2000; Lane *et al.*, 2001]. Then the length of the interference pattern is the length of crack.

The circinal bonded wafers will generate curvilinear crack in the processing of external force. In order to get the parameters of the bonding strength, the geometrical parameters of the crack region must be calculated first. After adjusting the accurate position of the razor and the wafers, the mask image can be gained with infrared system as shown in Fig. 9. Here the razor blade touches the gap of the wafers. As the razor inserting, the interference pattern generates gradually and the image after the razor inserted is shown in Fig. 10.

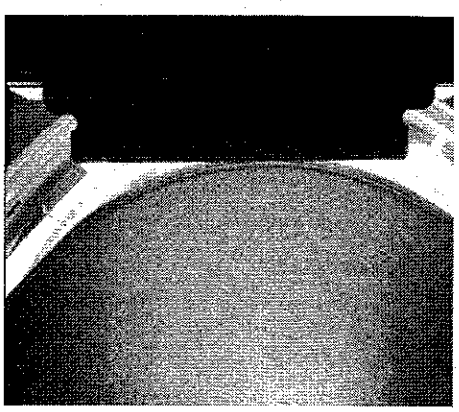

Fig. 9. Mask image before the razor inserting.

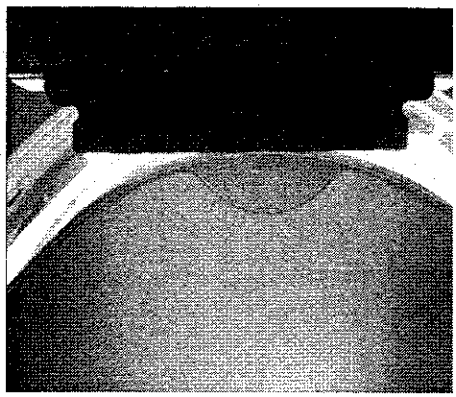

Fig. 10. Image after the razor inserting.

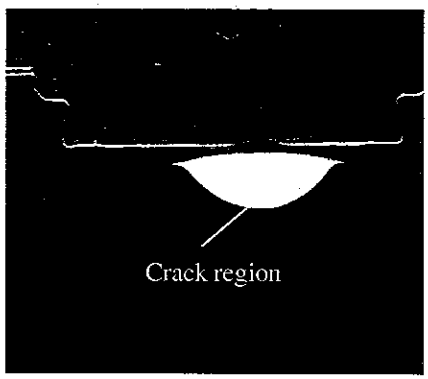

Fig. 11. Crack opening area measurement.

Contrasting Fig. 9 with the masked image of Fig. 10, the difference was generated by the motion of the razor and the growth of the crack region. Subtracting the mask image from Fig. 10 and segmenting the result image with an appropriate threshold, the crack region and the razor's motion is divided as in Fig. 11. Using area filtering compares the connected regions in the binary image, the maximal area can be considered as the crack region.

4. Experiments

4.1. *Experiment setup*

In the system the wafer is clamped vertically in the wafer clamper, which is mounted on the wafer adjustment stage. The razor is fixed vertically along the blade feeding stage surface. Driven by the positioning stage, the wafer can

be adjusted horizontally to align with the razor blade, and the razor can be fed with selected velocity inserting into the crack line.

The specimen must be mounted on a free rotation clamper, which is mounted on a precision positioning worktable named wafer adjustment stage to allow perfect alignment of the blade during testing. On the other hand, the inserting depth of the blade can be precisely controlled by another positioning modal named razor feeding stage to avoid damage to the specimen during testing.

4.2. *Experiment result*

A contrast experiment was carried out to test the feasibility of the system. The bonded wafers we used are about 100 mm diameter in size and 50 μm in thickness. A razor of 100 μm in thickness is used to insert into the crack line with constant velocity of 40 μm/s guided by microscopic subsystem. Two samples are respectively annealed at 150°C and 300°C for about 150 h. The image acquisition software is used in order to record the images and to evaluate the crack length continuously, and the inserting depth was gained through recording the position of the razor feeding stage.

Figure 12 shows the variation of the crack length as a function of the inserting depth for two annealed samples. Owing to the microscopic subsystem, the razor blade can be aligned precisely and the initial velocity of the blade insertion can be controlled, so the phenomenon appeared in initial zone reported in [Bertholet *et al.*, 2004] was avoided completely.

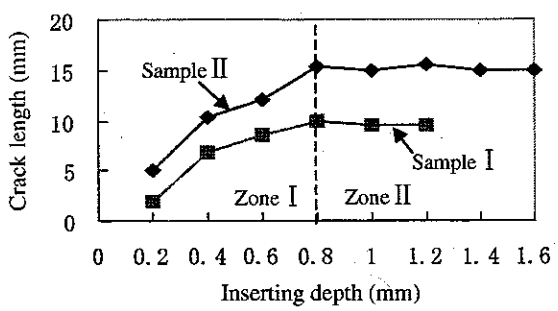

Fig. 12. Evolution of crack length during inserting the razor.

Two zones can be distinguished. In the first zone, the crack length increases with the inserting depth due to the isosceles triangle shaped razor tip. The second zone corresponds to the true steady-state regime giving relevant crack length values. Only crack length values belonging to this plateau will be considered in the determination of the bonding strength.

Two steady-state images are recorded by IR vision subsystem as Figs. 13 and 14.

The crack length was marked in the picture and measured as 4.612 mm and 7.654 mm. The bonding strength of the two samples was calculated respectively as 0.279 J/m^2 and 0.044 J/m^2. The area was the black region and computed as 66 mm^2 and 125 mm^2. The bonding strength of the two samples was calculated respectively as 0.833 J/m^2 and 0.116 J/m^2.

Some contrast experiments about crack length and crack area were carried out to test the bonding strength. The result was described by Fig. 15.

It was obvious that the strength calculated by area was bigger than that by length, since the crack length theory was universal, and it was inferred via quadrate wafers. However most wafers in practice were circular, so they must be amended. In fact, the denotative

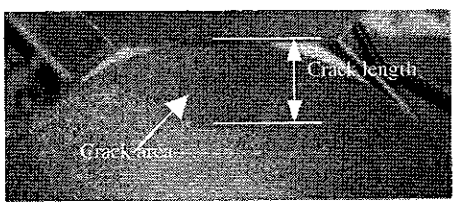

Fig. 13. Crack length and area image for sample.

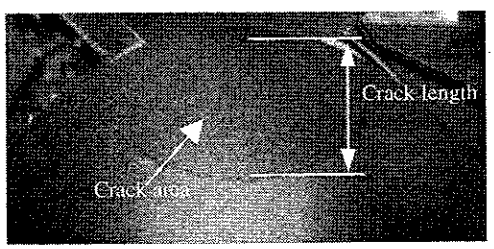

Fig. 14. Crack length and area image for sample II.

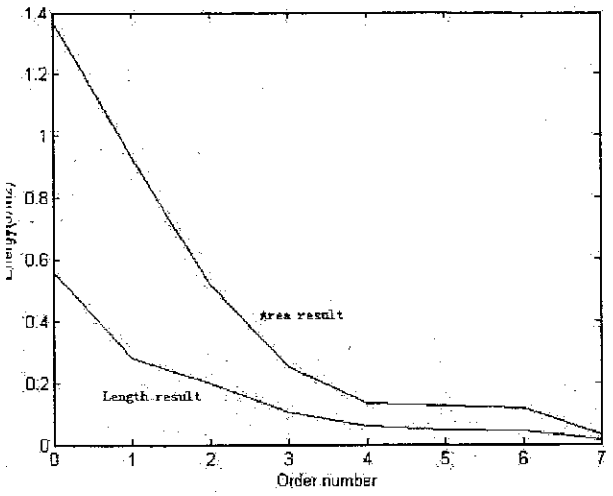

Fig. 15. The strength result of length and area.

Table 2. Measurement error.

Length (mm)	0.5	1	2	4	6	10
Error	10%	4%	2%	1%	0.7%	0.4%

area of crack length was more than the actual crack area.

5. Error Analysis

Through analysis of Eq. (15), the bonding strength are affected by the thicknesses of the razor and the samples, the diameter of the samples and the crack length. In the experiments, the metrical precision of the razor and the sample can be controlled as $0.5\,\mu$m. L is evaluated by IR system, and the minimal crack length measured by the IR system is $10\,\mu$m. So the measurement error of bonding strength is generated primarily by the measurement error of crack length L. The detail values are given in Table 2.

So, as long as the crack length generated in the experiment is larger than 4 mm, 1% measurement error of the bonding strength can be gained through this method.

6. Conclusion

The bonding strength is the technology index which can evaluates the quality of bonding strength. It has a significant process to improve upon the bonding techniques. In this paper, the measurement system of bonding strength based on crack-opening method was designed. Guided by microscopic subsystem, the razor blade was aligned to the crack line precisely and the razor tip shape was measured too. The razor can be inserted into the crack line steadily, which assures the precision measurement of the crack length with IR vision subsystem. The toughness of the bonded wafers has been measured with this system and the feasibility of the system was tested through experiments.

Indeed, if the bonding strength is greater than the toughness of the substrate, the crack will propagate into the substrate and preventing to the measurement of the cracking resistance of the interface. So, this type of test does not allow measuring toughness values greater than the substrate toughness.

References

Barth, P. W. [1990] "Silicon fusion bonding for fabrication of sensors," *J. Actuators and Microstructures Sensors and Actuators* **A21–23**, 919.

Bertholet, Y., Ikerb, F., Raskin, J. P. and Pardoen, T. [2004] "Steady-state measurement of wafer bonding cracking resistance," *Sensors and Actuators* **A110**, 157.

Lane, M. W., Snodgrass, J. M. and Dauskardt, R. H. [2001] "Environmental effects on interfacial adhesion, Microelectron," *Reliability* **41**, 1615–1624.

Lasky, J. B. [1986] "Wafer bonding for silicon on insulator technologies," *J. Appl. Phys. Lett.* **148**(1), 78–80.

Lawn, B. [1993] *Fracture of Brittle Solids*, 2nd ed., *Cambridge Solid State Science Series*, Cambridge University Press, Cambridge.

Maszara, W. P., Goetz, G., Caviglia, A. and McKitterick, J. B. [1988]. "Bonding of silicon wafers for silicon-on-insulator," *J. Appl. Phys.* **64**, 4943–4950.

Piotrowski, T. and Jung, W. [2000] "Characterization of silicon wafer bonding by observation in transmitted infrared radiation from an extended source," *Thin Solid Films* **364**, 274–279.

Tong, Q. Y. and Gösele, U. [1999] *Semiconductor Wafer Bonding: Science and Technology*, Wiley, New York.

Tong, Q. Y. [2001] "Wafer bonding for integrated materials," *J. Materials Science and Engineering* **B87**, 323–328.

Tvergaard, V. and Hutchinson, J. W. [2006] *The Relation Between Crack Growth Resistance and Fracture Process Parameters in Elastic-plastic Solids.*

Biography

Liguo Chen received his PhD in mechatronics engineering from Harbin Institute of Technology, Harbin, China. He is currently an associate professor at Robotics Institute, Harbin Institute of Technology. His research interests include micromanipulation robot, micro-actuator technique, robot vision technique.

Tao Chen received his BSE and MSE in mechatronics engineering from Harbin Institute of Technology, Harbin, China. He is currently pursuing his PhD in Robotics Institute, Harbin Institute of Technology. His research interests include micromanipulation robot for MEMS.

Lining Sun received his PhD in mechatronics engineering from Harbin Institute of Technology, Harbin, China. He is currently a professor at Robotics Institute, Harbin Institute of Technology. His research interests include micromanipulation robot, micro-actuator technique, medical robot and micro-robot.